science for a changing world

Methods and Spatial Extent of Geophysical Investigations, Mono Lake, California, 2009 to 2011

Open-File Report 2013–1113

U.S. Department of the Interior
U.S. Geological Survey

FRONT COVER:
Map showing location of seismic tracklines in Mono Lake: 2009 (solid lines), 68 tracklines, total 318 km; 2011 (dashed lines), 60 tracklines, total 199 km. Map prepared by Florence Wong, USGS Coastal and Marine Geology.

Methods and Spatial Extent of Geophysical Investigations, Mono Lake, California, 2009 to 2011

By A.S. Jayko, P.E. Hart, J.R. Childs, M.H. Cormier,
D.A.Ponce, N.D. Athens, and J.S. McClain

U.S. Department of the Interior
SALLY JEWELL, Secretary

U.S. Geological Survey
Suzette M. Kimball, Acting Director

U.S. Geological Survey, Reston, Virginia: 2013

Acknowledgments

Contents

Figures

Methods and Spatial extent of Geophysical Investigations, Mono Lake, California, 2009 to 2011

By A.S. Jayko[1], P.E. Hart[2], J.R. Childs[2], M.H. Cormier[3], D.A.Ponce[2], N.D. Athens[2], and J.S. McClain[4]

Abstract

This report summarizes the methods and spatial extent of geophysical surveys conducted on Mono Lake and Paoha Island by U.S. Geological Survey during 2009 and 2011. The surveys include acquisition of new high resolution seismic reflection data, shipborne high resolution magnetic data, and ground magnetic and gravity data on Paoha Island. Several trials to acquire swath bathymetry and side scan sonar were conducted, but were largely unsuccessful likely due to physical properties of the water column and (or) physical properites of the highly organic bottom sediment.

Introduction

Mono Lake, a saline lake with ashoreline elevation of about 1945–1950 m, lies in the rain shadow of the Sierra Nevada in eastern California. The historical lake level has fluctuated in response to both seasonal precipitation and water diversion via the Los Angeles aqueduct (Pelagos Corporation, 1987). The lake is elongated and currently about 18–19 km by 13.5 km, with a surface area of about 200 km^2 (fig. 1). The morphology of the lake bottom is irregular and reaches depths of ~51.5 m in Putnam Basin due east of Paoha Island, but otherwise has an average depth of about 18 m (Scholl and others, 1967, Raumann and others, 2002). The lake bottom has been significantly modified by late Holocene igneous activity, including magmatic intrusion and eruptions that formed Paoha Island and the Negit Island archipelago.

Mono Lake basin lies north of Mammoth Mountain, a late Quaternary volcano that lies along the southwest margin of Long Valley Caldera and due south of the Mono-Inyo volcanic chain (Hill and Prejean, 2005). Mono Lake basin contains a chain of volcanoes that includes the northern part of the Inyo-Mono craters, Oh Ridge basalt, Black Point basalt, and volcanoes of the Mono Lake islands. These Holocene and Late Pleistocene craters, obsidian domes, intrusions, and vents extend northward from the north moat of Long Valley Caldera to the northwest corner of Mono lake (Hildreth, 2004, fig. 1). Both the north and south ends of the Inyo-Mono craters have been active within the past 300-600 years and several small vents and intrusions formed islands within the lake during late Holocene time (Huber and Rinehart, 1967; Scholl and others, 1967; Wood, 1983; Sieh and Bursik, 1986; Bursik and Sieh, 1989; Stine, 1990).

---

[1]U.S. Geological Survey, 3000 East Line St., Bishop, CA., 93514
[2]U.S. Geological Survey, 345 Middlefield Road, Menlo Park, CA., 94025
[3]University of Missouri, Columbia, MO
[4]University of California Davis, Davis, CA
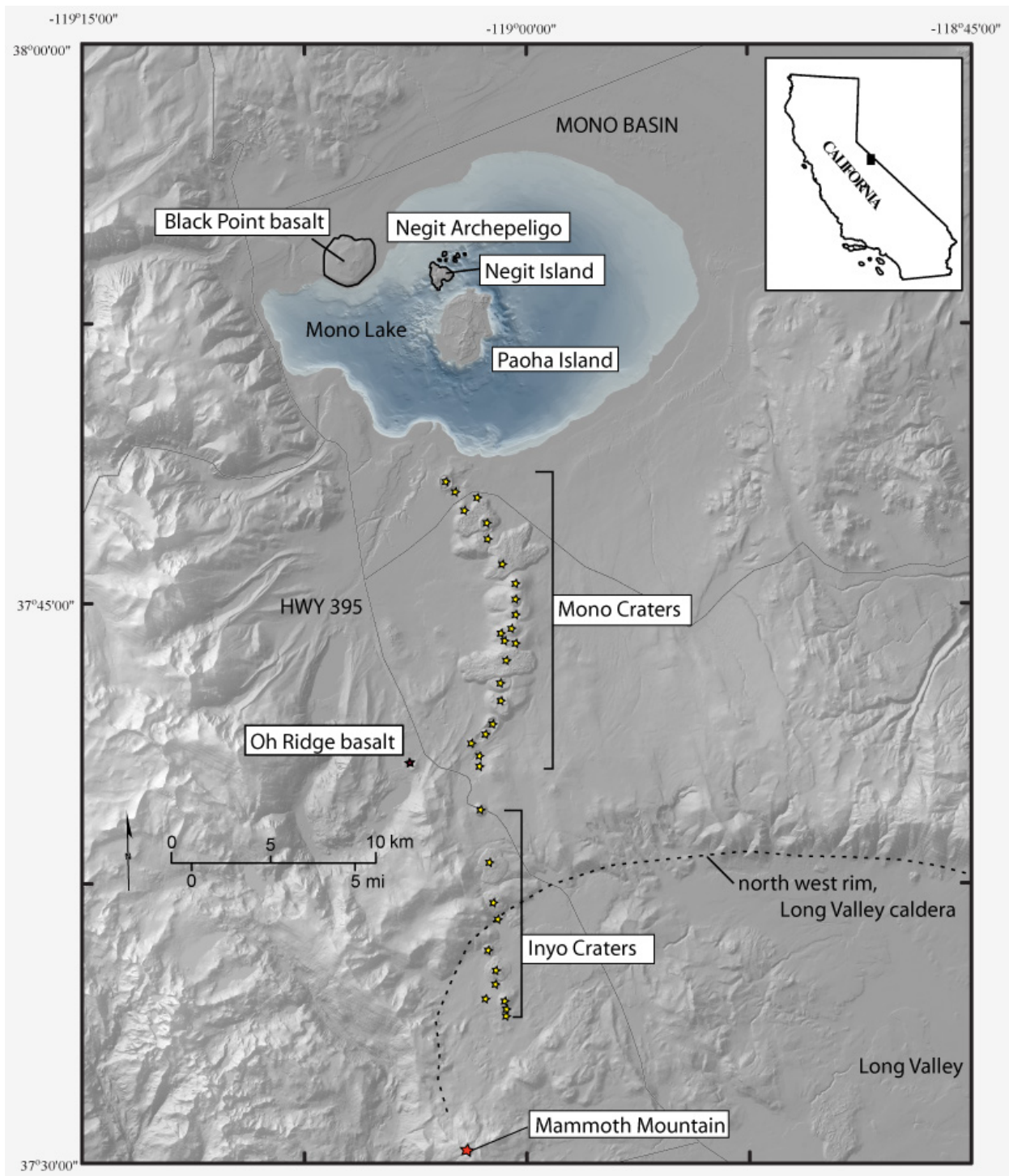
Figure 1. Map showing the location of Mono Lake, its islands, Inyo-Mono Craters and Mammoth Mountain. Stars indicate locations of eruptive centers/vents.

     The last effort to collect sub-bottom data using geophysical techniques occurred almost 25 years ago (see below). Improvements in instrumentation, Global Positioning Systems (GPS), and data processing, warrant a new iteration of ship-borne geophysical data collection. Accordingly, in 2009–2011, offshore geophysical surveys were conducted in Mono Lake to gain a better understanding of the

basic late Quaternary subbottom structure and bottom deposits, with the expectation of learning more about the timing and extent of volcanic eruptions and their relation to active faulting beneath the lake. The surveys were also conducted to acquire new basic understanding of the lacustrine bathymetry that could be used for geomorphic analysis of glacial-fluvial-deltaic deposits and submerged strandlines beneath the current, historically low shoreline. The initial emphasis of the offshore geophysical work (2009–2010) was to collect high-resolution seismic reflection data, swath bathymetry, and sidescan sonar data for analysis and public-domain access. This was followed up in 2011 with acquisition of high-resolution ship-borne magnetic and ground-based gravity data. Additional seismic reflection data were also collected during 2011 in areas of good data quality and high geologic interest.

The objective of this report is to summarize information about methods and extent of the 2009 and 2011 geophysical surveys on Mono Lake. These efforts were, in part, pilot studies intended to provide direction for future efforts. Not unexpectedly, acoustic imaging of the lake floor and subbottom was unsuccessful over substantial areas owing to the physical properties of the lake bottom (for example, highly organic deposits with disseminated gas, and (or) highly organic lake water with elevated temperature, and total dissolved solids (TDS) stratification in the water body). Data, results and data synthesis will be released in other reports associated with ongoing investigations of active faulting and volcanism.

Previous Offshore Geophysical Studies and Related Work

Previous offshore geophysical studies were conducted by Scholl and others (1967) and by Pelagos Corporation, San Diego (1986–1987) under contract with the Los Angeles Department of Water and Power. Scholl and others (1967) collected acoustic profiling data; Pelagos collected bathymetric, seismic reflection, video, and photographic data, as well as sound velocity measurements and 50 bottom samples. Bathymetric maps of the lake were produced from both studies, with denser line spacing, more accurate navigation, and higher resolution data collected in the more recent effort by Pelagos Corp. The Pelagos Corporation (1987) bathymetric data were subsequently digitized, converted to a raster elevation model, and released as a USGS Miscellaneous Field Studies Report by Raumann and others (2002).

Scholl and others (1967) recorded bathymetry along ~322 km (~200 mi) of acoustic profiling lines using a continuously recording 38-kHz fathometer. Locations were determined using two simultaneous horizontal shipboard sextants shot to benchmarked sighting stations onshore and recorded about every 5 minutes. They reported the velocity of sound in Mono Lake as 1,545 m/s (5,069 ft/s) and depths accurate to 0.15 m (0.5 ft). The resulting bathymetric data were contoured at ~3 m (10 ft) and published at 1:62,500 scale. They observed the presence of acoustically "translucent" sediment that overlies a "main" subbottom reflector and constructed a basin wide isopach map of the translucent sediment thickness.

Scholl and others (1967) also made several important additional physical and geologic observations. They noted: (1) freshwater artesian springs on the lake bottom that lowered the acoustic velocity by as much as 6.3 percent, causing local apparent deepening of the bottom; (2) hummocky bottom, locally with a thin sediment fill, near Negit Island that they ascribed to sublacustrine lava flows; (3) deformed Pleistocene lake sediment; (4) a bathymetric lineament that passes under Negit Island colinear with the northern shoreline and is likely an expression of one of the major basin-defining faults; (5) a submerged terrace that they interpreted as a possible submerged shoreline from the Altithermal event about 4,000 years ago; (6) the relative youthfulness of both Negit and Paoha Islands, which they speculate based on geomorphic evidence may be several thousand to only several hundred years old; and (7) that most of the large-scale and small-scale bathymetric features are probably recent rather than last glacial (Tioga) age based on relative geologic and geomorphic position.

Between September 1986 and February 1987, Pelagos Corporation (now Racal Pelagos, hereafter referred to as Pelagos), under contract to Los Angeles Department of Water and Power, collected 1,020 line km (634 line mi) of bathymetric and high resolution geophysical data from the following instruments: two frequency echo-sounders, the Raytheon DE719 (208 kHz) used in shallow water less than 15 m (50 ft) and the DE731 (40 kHz) used in both deep and shallow water; Ferranti O.R.E. GeoPulse (boomer-type) single channel subbottom profiler; Ferranti O.R.E. Model 1500 sidescan M160 transceiver with M158 tow fish sonar with 100-kHz beams; and Motorola Mini-Ranger III GPS for navigation. Vessel speed was generally 4.0 knots or slower around islands and shallow water. The lake level at the time of data collection was ~1,944.8 m (6,380.7 ft) elevation. Sound velocity measurements were taken twice a day using Sippican XSV-03 expendable sound-velocity probes. Considerable variation in the speed of sound was found throughout the lake. Most the variation occurred within the upper 3 m of water depth, and acoustic velocity became effectively constant below 12 m. Depth data were originally recorded assuming a constant velocity of 1,463 m/s (4,800 ft/s), and subsequently some adjustments were reportedly made based on these data. The 100-kHz sidescan was able to image the lake bottom, although the Pelagos report noted that the sidescan sonar "could not achieve the same ranges attainable in a fresh- or sea-water environment" (Pelagos, 1987).

Pelagos Corporation generated local sediment isopach maps for parts of the basin, a map of geologic bottom features, geologic cross-sections, and bathymetric maps at 1:6,000 scale with 2-foot contour interval and at 1:12,000 and 1:24,000 scales with 5-foot contour interval. The bottom feature/material map was primarily generated from sidescan sonographs with confirmation by diver observations, diver photographs, and bottom samples. Pelagos Corporation noted two acoustic reflectors labeled A and B beneath the "translucent sediment' or ooze. Horizon A occurs at 0–12 m (0–40 ft) below the lake bottom, and Horizon B occurs at 3–12 m (10–40 ft) below the lake floor. They found no direct stratigraphic correlation between Horizons A and B. The translucent sediment ooze was as much as 18 m (60 ft) thick in Johnson Basin, consistent with the >12 m (40 ft) thickness reported there by Scholl and others (1967). They also found scarps and (or) lineaments in the area noted by Scholl and others (1967), north of Simon Spring where Bursik and Sieh (1989(found a scarp onshore, and offshore from the Mono Lake Fault (Bursik and Sieh, 1989) in the area north of the Lee Vining delta.

The USGS collaborated in the Pelagos survey in 1986 by recording several Uniboom lines Images of the Uniboom records are available at:
http://walrus.wr.usgs.gov/infobank/m/ml186ca/html/m-l1-86-ca.meta.html.

USGS acquired the Pelagos bathymetric data (as contours, not soundings) for the purpose of producing a digital elevation model (DEM) of the lake bottom. Point elevations in State Plane coordinates (North American Datum of 1927) were digitized from topographic sheets. In addition, the contour maps from the Pelagos Corporation (1987) report were scanned, and contour lines were digitized as vectors (lines/arcs). Some elevation point corrections and additions were made in the vicinity of the Negit Island islets. Arcinfo TOPGRID command was used to interpolate the vectorized contour data (arcs) which were exported at 10-m grid spacing. The 10-m grid elevation model was published in ARC/GRID format by Raumann and others (2002).

Geophysical Surveys 2009–2011

Overview
High-resolution seismic reflection surveys were conducted from August 30 to September 5, 2009, and from September 7 to 15, 2011, using a minisparker sound source and a single-channel hydrophone receiver cable towed approximately 20 m behind the University of California Davis 22-foot

research trawler *Vandel* (fig. 2). Sidescan sonar data were collected September 8 to 11, 2009, in shallow water (~10 m or less) using a Klein 3900, 445-kHz fish with electric winch for towing at depth. Two trials, in September and October 2010, were conducted to assess the feasibility of mapping the lake bottom high-resolution swath bathymetry. The results of these trials (described below) suggested that the swath mapping instrument would not work in Mono Lake. Offshore high-resolution magnetic data were collected from August 25 to September 6, 2011, using a Geometrics G858 magnetometer mounted on the *Vandel*. Ground-based magnetic data were collected from August 26 to September 5, 2011 on Paoha Island using a Geometrics G858 magnetometer. Ground-based gravity data were collected August 26 to September 5, 2011, on Paoha and Negit Islands using a Scintrex CG-5 gravity meter and Geometrics G858 magnetometer.

Navigational positioning for all boat surveys was acquired with differential GPS (WGS-84) using a CSI DGPS Max using WAAS correction. No post processing was performed on the navigation data. Horizontal accuracy is estimated to be within 1 meter (at 95 percent confidence level.

Sparker Seismic Reflection Profiling 2009 and 2011

A total of 517 km of subbottom seismic reflection profile tracklines were collected August 30 to September 5, 2009, and September 7 to 15, 2011 (fig. 3). Both surveys were conducted at survey speed of between 4 and 5 knots using an Applied Acoustics CSP-D minisparker with a 1-m-long, 50-tip source (fig. 4) and a Geopulse 5-m, 30-element single-channel hydrophone streamer, both towed at ~1 m depth. The midpoint of the source and receiver were approximately 20 m aft of the GPS antenna on the *Vandel*. Data were not corrected for layback. In 2009, the minisparker was operated at 200 joules emission; record length was 230 to 275 ms; and shot interval 250 or 300 ms. In 2011, the minisparker power was 300 joules; the record length 300 ms; and shot interval 350 ms. Data were digitally recorded at 10 kHz with a Triton Sub-bottom Logger (SBL) system. The digital SEG-Y files were loaded into Seisworks seismic interpretation package, and converted to depth using a P-wave velocity of 1,450 m/s. 10 ms two-way travel time (TWTT) is estimated to correspond to approximately 7.25 m in depth. Although the survey line spacing was variable, depending on location and geologic features of interest, much of the lake was covered at a line spacing of 0.65 to 0.5 km or closer (fig. 3).

During the 2009 survey, lake level was at approximately 1,945.2 m (6,382 ft), and during the 2011 survey it was 1,945.8 m (6,384 ft.), according to records available at: *http://www.monobasinresearch.org/data/levelyearly.htm.*

Subbottom data-imaging penetration was variable, depending on physical condition of the sediment—primarily on the acoustic blanking effects caused by the likely occurrence of interstitial gas bubbles. The deepest acoustic penetration reached about 50 to 75 m subbottom in some nearshore areas, but offshore it commonly only reached 10 to 15 m. Large areas of gas-saturated sediment, as well as mid to late Holocene landsliding around igneous domes, flows, and vents, were significant factors limiting image quality. Figure 5 shows a representative example of data collected in shallow water depths, displaying prominent dipping reflectors on the left side of the profile to subsurface depths of almost 40 meters.

Figure 2. The 22 foot University of California Davis trawler *Vandel* on Mono Lake.

Data interpretation is complicated by the occurrence of dramatic lateral changes in acoustic character of the sediments. We hypothesize that these changes are the result of changes in free-gas pore content of the sediment. Where the gas saturation reaches a certain threshold, interstitial bubbles form and the reflection character abruptly changes (fig. 6). This phenomenon is commonly observed elsewhere, for example in San Francisco Bay (Marlow and others, 1996) and in gas-charged sediments in Tierra del Fuego (Lodolo and others, 2012).

Georeferenced maps showing location of these seismic reflection survey track lines are available at:

(2009) *http://walrus.wr.usgs.gov/infobank/v/v109ca/html/v-1-09-ca.meta.html;*

(2011) *http://walrus.wr.usgs.gov/infobank/v/v0111ca/html/v-01-11-ca.meta.html.*

Swath Bathymetry Trials in September and October 2010

In 2010, trial surveys were conducted to evaluate the feasibility of mapping Mono Lake with a swath bathymetric mapping system. The swath-mapping instrument was an SEA (AP) Ltd. SWATHplus phase-differencing ("interferometric") side-scan sonar, which operates at variable frequencies of 117, 234, and 468 kHz . This instrument has been used both inland and offshore to map water depths less than 200 m. (See, for example, Ritchie and others, 2010; Finlayson and others, 2010). For these trials, the sonar head was pole-mounted outboard of the gunnel of the *Frontier*, a 23-foot Whaler (fig. 7).
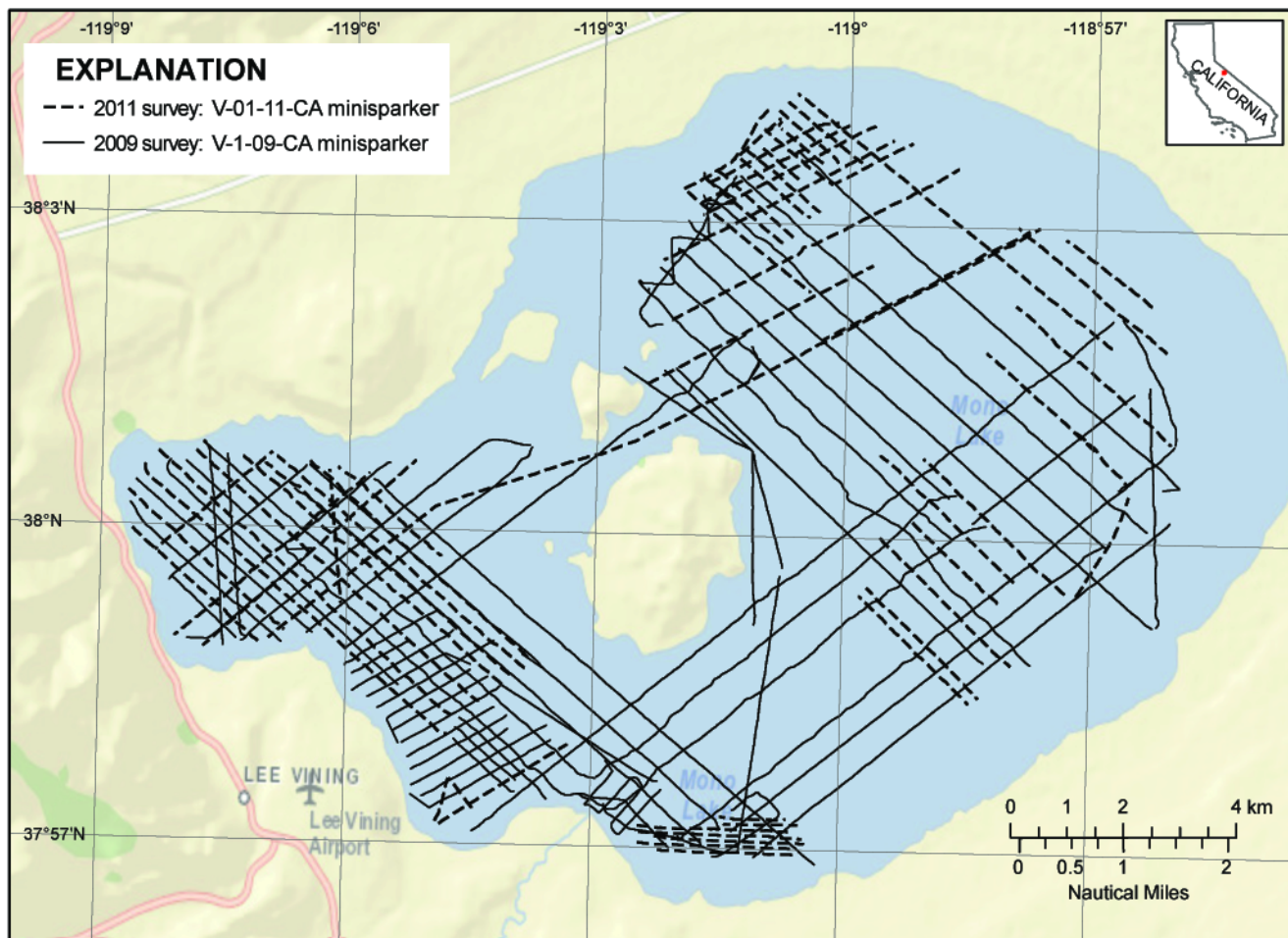
Figure 3. Map showing location of 2009 seismic tracklines in Mono Lake: 2009 (solid lines), 68 tracklines, total 318 km; 2011 (dashed lines), 60 tracklines, total 199 km.

The initial test survey, September 27 to October 1, 2010, employed the 234.5-kHz sonar transducer. The results of the test were discouraging—the maximum water depth that could be imaged was limited to 4 to 5 m and the swath width to 1 to 2 times water depth. (Under more typical conditions, swath width is as much as 15 to 20 times water depth.) The second trial was conducted a week later on October 8, 2010, using lower frequency 117-kHz transducer heads. Although the lower frequency resulted in increased propagation depth, the maximum depth was still limited to 8 to 10 m, and swath width was similarly limited. The single-beam fathometer, operating at 200 kHz, successfully operated over the entire depth range of the lake (down to 50 m), which is attributed to a much more focused, single transmission beam and a near-vertical travel path.

Reasons for the limited depth range and poor swath width are uncertain. We speculate that possible causes include a bottom "bio-fluff layer" of low acoustic impedance that returns very little energy; the extreme alkalinity of the lake that attenuates the signal; the alkaline water causing poor transducer "wetting;" and signal attenuation due to the acoustic scattering effect of a high volume of brine shrimp. Further speculation on the cause of the poor functionality of the side-scan and swath instruments is found in the side-scan discussion below. These results are similar to those observed using

7

Figure 4.   Minisparker 50-element source (approximately 1-meter long) at the end of its cable.

a similar high-frequency (445 kHz) Klein 3900 side-scan sonar. This instrument operated in only the shallowest areas of the lake and returned limited-resolution images. Pelagos (1987) also reported limited success using a 100-kHz Ferranti O.R.E. Model 1500 side-scan system. The sonar could not image reflectors beyond a water depth of 75 m, and in the deeper areas of the lake "very little reflected energy was returned". After review of other side-scan technology available at the time, Pelagos concluded that "no other system on the market could produce better results or obtain greater ranges than the O.R.E. system being utilized."

In view of the very limited depth range, the swath trials were abandoned, and no further testing is planned. Although theoretically a swath system operating at much lower frequency (for example, 12 kHz) and higher power could be used to map the lake, these systems are proportionally larger in both size and weight and would not be feasible to deploy from a small boat.

High-Resolution Sidescan Survey, 2009

The sidescan sonar used to survey Mono Lake was a high-resolution Klein 3900, a digital, dual-frequency sidescan with a nominal swath width of 300 m at 445 kHz, and 100 m at 900 kHz. Sidescan mosaic images were produced using the software package SonarWiz from Chesapeake Technology. The intention was to illuminate the lake in its entirety and to precisely image submerged tufa towers, lava flows, landslides, fissures, and fault scarps.
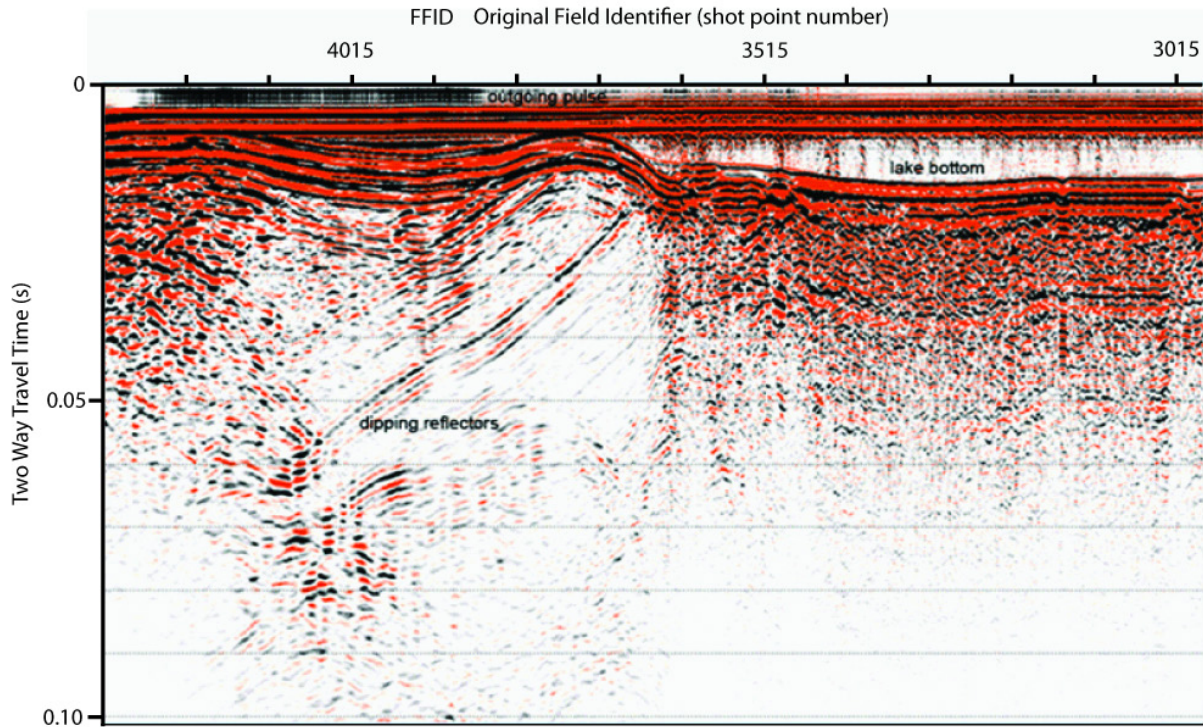
Figure 5.   Mono Lake minisparker line 26, located in the north east part of the lake, illustrating dipping reflectors visible to almost 40 meters subbottom, in water depth ranging from approximately 6 to 11 meters.

Deployment occurred during the second week of September 2009 and revealed two unexpected problems with the sidescan sonar. One was that the port (left) side produced nearly no returns—a defect with the sonar equipment. The other issue was the extreme signal attenuation for both sonar frequencies, even for the functional starboard (right) side. After experimenting with towing depths, it became clear that useful data could be recorded only when the sonar was towed 1 to 2 m above lake bottom and that, in that case, the swath width would be 15 m to each side, at best. Survey speeds ranging from 1 to 3.5 knots all produced similarly poor results.

Because of these limitations, the survey strategy was revised to focus on five small areas, each roughly 1 to 2 km long and 50 to 100 m wide, with a track spacing of 25 to 30 m. These subareas are located in figure 8. Two subareas near Negit Island were selected to image possible lava flows (north of Negit Island) and a landslide inferred from the minisparker survey (west of Negit Island).   The survey north of Negit Island did not produce useful imagery, possibly because of a smooth featureless bottom. The survey west of Negit Island (fig. 9) reveals a mottled bottom in the northern half that suggests algal mats but the southern half appears featureless, possibly because of a smooth, undisturbed sediment cover. A survey near the north shore of the lake was designed to image the possible underwater extension of a north-northeast-striking fault that was tentatively mapped onshore. That survey did not detect any lineament aligning in a north-northeast direction, but it did map numerous tufa towers. It also imaged a gas plume that bubbled to the lake surface (fig. 10). A tufa tower does not appear to be associated with that seep, but rather the bubbles emanated directly from the lake bottom at a water depth of about 3 m (fig. 11). The survey near the east shore of the lake was designed to image the possible underwater extension of a roughly north-south-striking fault (Bursik, 1989). Survey tracks were oriented parallel to a bathymetric escarpment visible in the digital bathymetric map (fig. 8; Raumann and others,

9
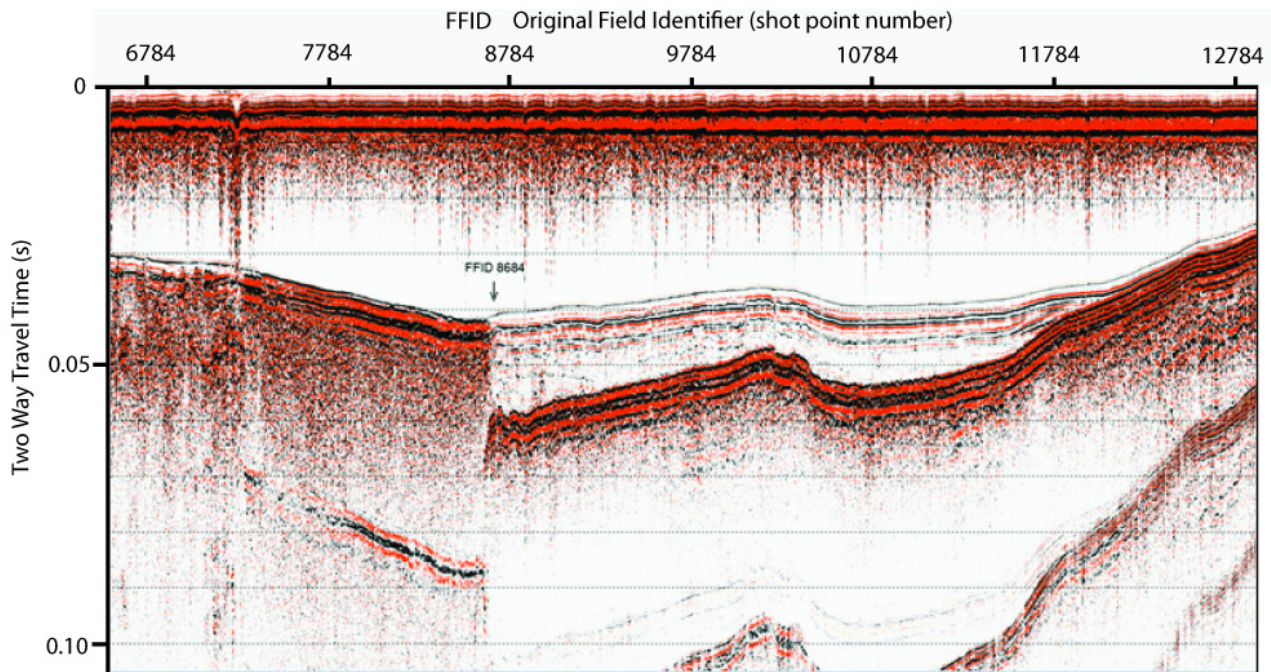
Figure 6. Mono Lake minisparker line 27, south central part of lake, illustrating the dramatic change in reflection character of the lake sediments at point FFID 8684. Continuous lake bottom is at approximately 0.04 seconds (two-way travel time), with prominent subbottom reflector visible at approximately 0.06 second. These dipping horizons are completely masked at FFID 8684 due to inferred higher gas concentration in the sediment which absorbs the acoustic energy.

2002). However, the mosaic does not reveal any lineament that might be associated with faulting, although the lake bottom here is mottled, possibly a result of sediment waves and (or) algal mats.

We speculate that reasons for the poor performance of the sidescan sonar might include the following. First, during the "typical" monomixic conditions that applied in 2009, the lake waters would have been highly stratified by summer time, with a thermocline/chemocline lying at a water depth of around 12–20 m (see, for example, Melack and Jellison, 1998). The pronounced thermal and chemical stratifications likely resulted in a dramatic upward-turning refraction of the acoustic signals at larger grazing angles, possibly preventing them from reaching the lake bottom. Second, even with the sonar towed below the thermocline/chemocline, the unusually high salinity of Mono Lake (about three times the average salinity of the oceans) may contribute significantly to acoustic attenuation at the high operating frequencies of the Klein 3900 sonar (see, for example, Richards, 1998), an effect that is more pronounced for higher frequencies. Lastly, the high abundance of brine shrimps and alkali flies in the lake during the summer months would contribute to scattering and dissipating the acoustic energy (see, for example, Richards, 1998; Jenkinson and Sun, 2010).

A successful strategy for future sonar surveys in Mono Lake might be to schedule acquisition in early spring (before April) or mid to late fall (after October), when the lake is not stratified and brine shrimps and alkali flies are not present. The use of sonars operating at lower frequencies than those of the Klein 3900 (around 100 kHz rather than 445–900 kHz) would likely help as well.

Figure 7. The *Frontier*, a 23-foot Whaler with SwathPlus transducer pole-mounted over the side.

Magnetic and Gravity Surveys, 2011

Introduction

From August 26 to September 5, 2011, the USGS collected more than 600 line-kilometers of ship-borne magnetic data on Mono Lake, 20 line-kilometers of ground magnetic data on Paoha Island, and more than 50 gravity stations on Paoha and Negit Islands (fig. 12). Magnetic and gravity data were collected to study regional crustal structures, both as an aid to understanding the geologic framework of Mono Lake and for their implications on potential geothermal resources and volcanic hazards throughout Mono Basin.

Ship-Borne Magnetic Data

About 626 line-kilometers of ship-borne magnetometer data were collected along approximately northeast- and northwest-trending traverses shown in figure 12. Magnetometer and Global Positioning System (GPS) data were collected simultaneously at 1-s intervals using a Geometrics G858 cesium vapor magnetometer attached to wooden and aluminum pole that extended the sensor about 2 m forward of the bow. The height of the magnetometer above the water surface was about 1 m. A portable Geometrics G856 proton-precession base-station magnetometer was used to record diurnal variations of the Earth's magnetic field during the ship-borne magnetometer surveys.

During field operations, ship-borne magnetic data were recorded and viewed in real time using Geometrics MagLog software. Raw magnetic data were downloaded and processed using Geometrics MagMap2000 software that merged magnetometer and GPS data. The location of the magnetometer was recorded using a Trimble nonmagnetic Ag132 GPS receiver mounted on an aluminum frame attached to the cabin of the boat. The Ag132 receiver has real-time differential correction capabilities using an Omnistar satellite system, resulting in submeter horizontal accuracy. The magnetic data in nanotesla
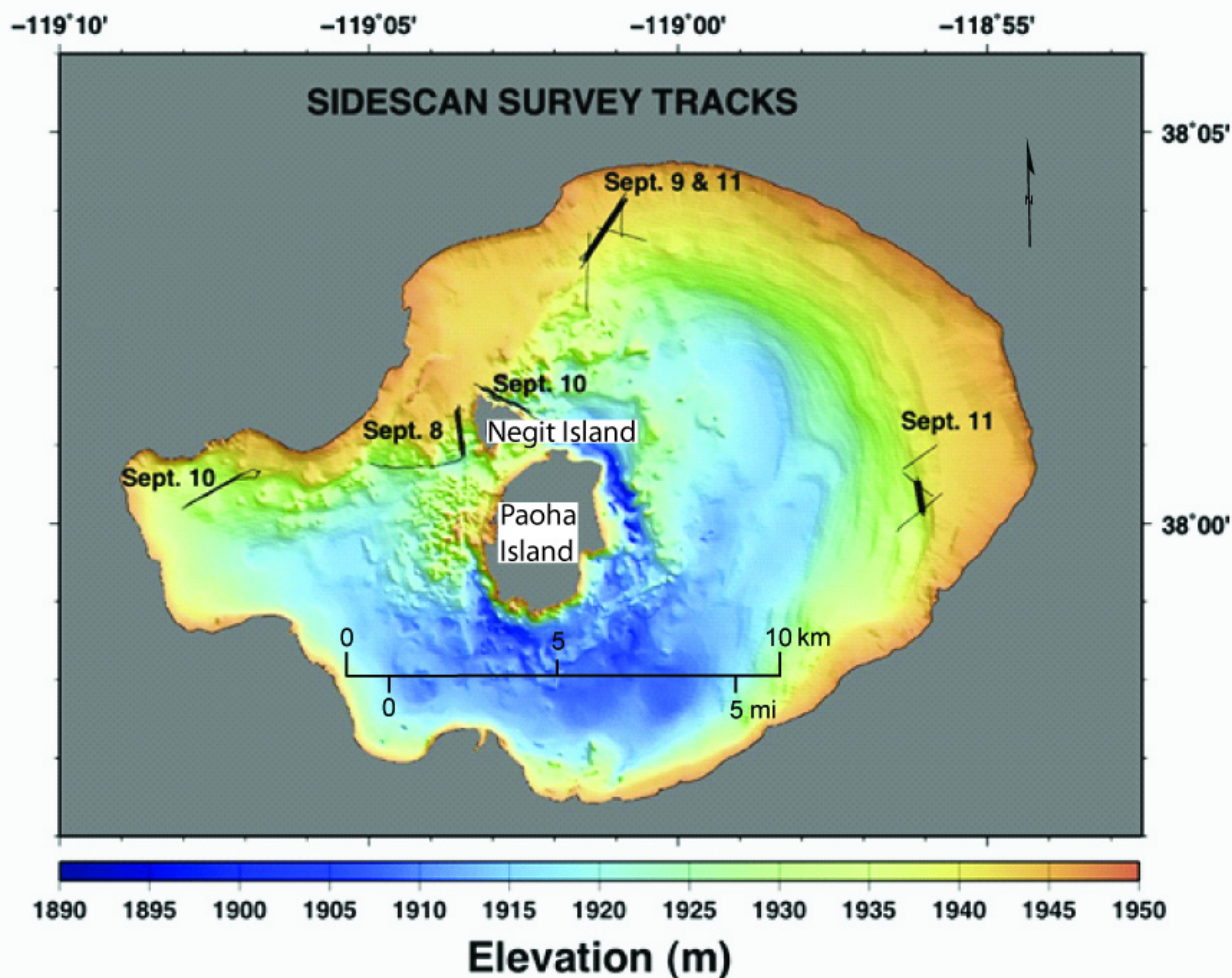
Figure 8. Tracks of the sidescan surveys done in five small subareas in Mono Lake in September 2009, overlaid on USGS bathymetric base map (Raumann and others, 2002). Thick lines represent multiple subparallel traverses; thin lines are single traverses. Date of data collection indicated near track lines. Lake surface elevation ~ 1944 m (6380').

(nT) units were collected in geographic coordinates. Diurnal variations of the Earth's magnetic field were recorded at a ground magnetic base-station near the boat launch on the western shore of the lake at Tioga Lodge by the Lake. Ship-borne data were corrected for diurnal variations, leveled, and corrected for vessel heading effects of the boat's magnetic field.

Ground Magnetic Data

About 22 line-kilometers of ground gradient magnetic data were collected along six approximately northeast-trending traverses across Paoha Island (fig. 12). These traverses were collected using a Geometrics G858 cesium vapor magnetometer with the same survey and GPS specifications as the ship-borne magnetometer surveys. The height of the magnetometer above the ground surface was about 2 m. A portable Geometrics G856 proton-precession base-station magnetometer was used to record diurnal variations of the Earth's magnetic field during the ground-magnetic surveys. Diurnal variations recorded by the base-station magnetometer were removed and the data were filtered to remove cultural noise. Individual lines were not leveled with one another.
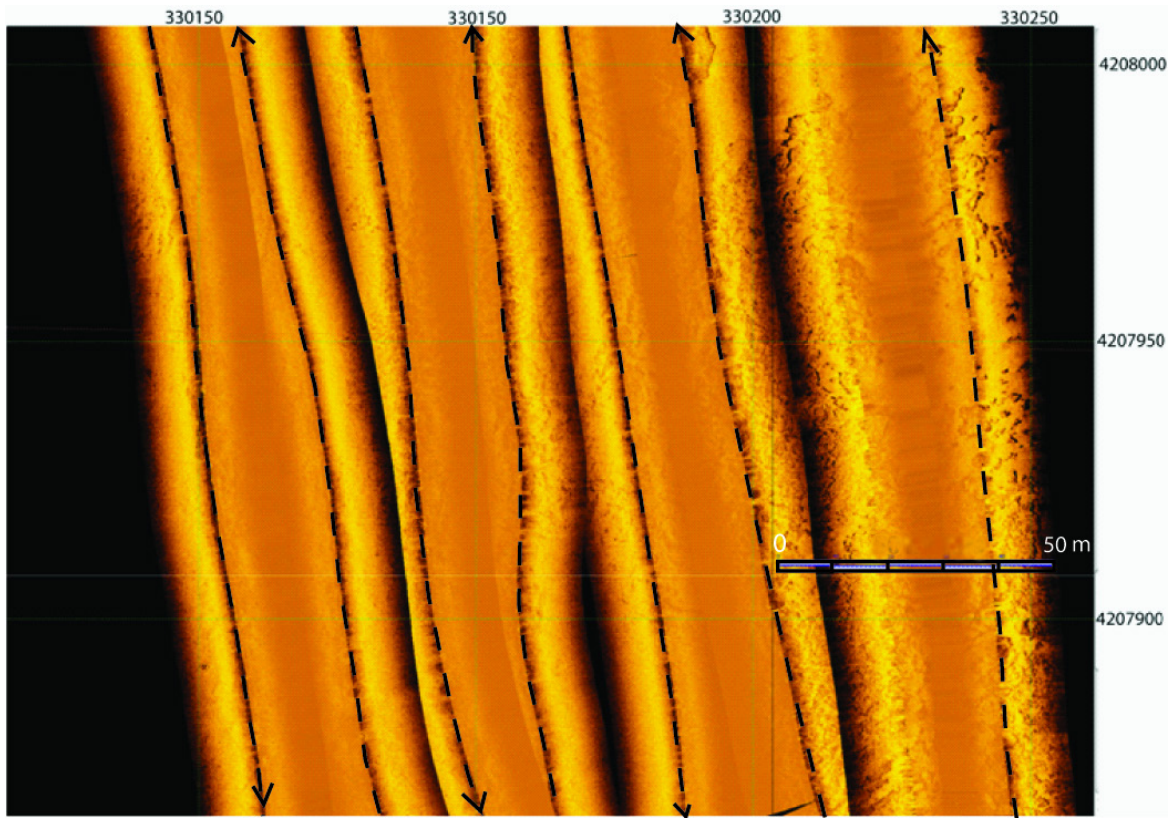
Figure 9. Detail of the high resolution sidescan mosaic collected Sept 8, 2008. Acoustic shadows are displayed in black. Both starboard and port side of the sidescan imagery are displayed and the darker stripes striking NNW correspond to the nadir below the instrument. However, the port (left) side was defective and did not produce useful return; the port side corresponds to the nearly featureless swaths in darker orange shades. Survey lines were run north and south; dashed lines show approximate ship track, arrow indicates tow direction. The mottled texture of the lake bottom is interpreted to be produced by discontinuous algal mats.

Gravity Data

Gravity data were collected along approximately northeast-trending traverses and consist of 56 new stations on Paoha and Negit Islands (fig. 12). All gravity data were tied to a primary base-station (LEEVIN) at the U.S. Post Office in Lee Vining, California, at lat 37°57.34'N. and long 119°07.14'W. (NAD27) with an observed gravity value of 979,348.30 mGal. All gravity stations were located between lat 37°55' and 38°05'N. and long 119°00' and 119°05'W.

Gravity data were reduced using standard gravity methods (see, for example, Dobrin and Savit, 1988; Blakely, 1995) and included the following corrections: (a) earth-tide correction, which corrects for tidal effects of the Moon and Sun; (b) instrument-drift correction, which compensates for drift in the instrument's spring; (c) latitude correction, which accounts for the variation of the Earth's gravity with latitude; (d) free-air correction, which accounts for the variation in gravity owing to elevation relative to sea level; (e) Bouguer correction, which corrects for the attraction of material between the station and sea level; (f) curvature correction, which corrects the Bouguer correction for the effect of the Earth's curvature; (g) terrain correction, which removes the effect of topography to a radial distance of 167 km around the station; and (h) isostatic correction, which removes long-wavelength variations in the gravity field related to the compensation of topographic loads.

Figure 10. Photos of the bubble plume in the northern part of Mono Lake. Location of this bubble plume is indicated on the sidescan mosaic in fig. 11.

A Scintrex CG-5 gravity meter was used in this survey. Conversion of meter readings to gravity units for Scintrex CG-5 gravity meter were made using factory calibration constants, as well as a secondary calibration factor determined by multiple gravity readings over the Mt. Hamilton calibration loop east of San Jose, California (Barnes and others, 1969). Observed gravity values were based corrected for a time-dependent linear drift between successive base readings and were referenced to the International Gravity Standardization Net 1971 (IGSN 71) gravity datum (Morelli, 1974, p. 18). Free-air gravity anomalies were calculated using the Geodetic Reference System 1967 formula for theoretical gravity on the ellipsoid (International Union of Geodesy and Geophysics, 1971, p. 60) and Swick's (1942, p. 65) formula for the free-air correction. Bouguer, curvature, and terrain corrections were added to the free-air anomaly to determine the complete Bouguer anomaly at a standard reduction density of 2,670 kg/m^3. Finally, a regional isostatic gravity field was removed from the Bouguer field assuming an Airy-Heiskanen model for isostatic compensation of topographic loads (Jachens and Roberts, 1981) with an assumed nominal sea-level crustal thickness of 25 km, a crustal density of 2,670 kg/m^3, and a density contrast across the base of the crust of 400 kg/m^3. Gravity values are expressed in milligals (mGal), a unit of acceleration or gravitational force per mass equal to 10^{-5} m/s^2.
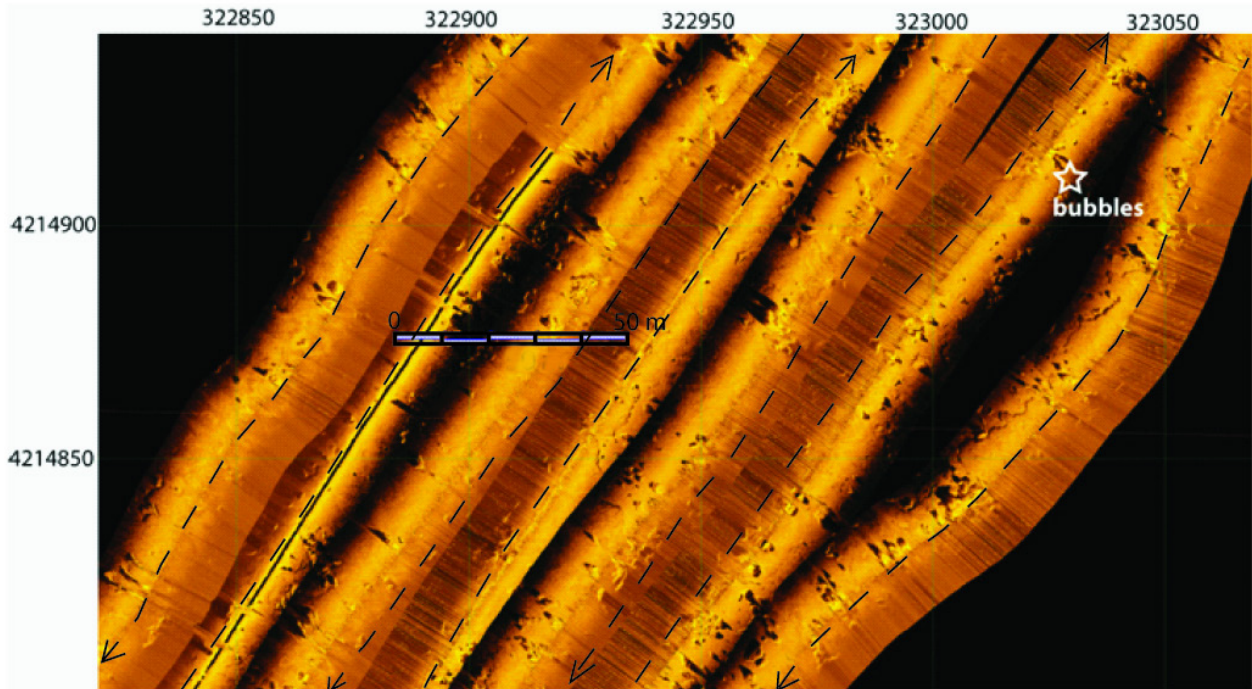
Figure 11. Detail of the sidescan mosaic collected Sept 9 and 10, 2009. Acoustic shadows, displayed in black, highlight tufa towers. The white star indicates the location of the bubble plume observed at the lake surface. The port (left) side of the sidescan was defective and did not produce useful return. Survey lines were run northeast and southwest; dashed lines show approximate ship track, arrow indicates tow direction. The mottled texture of the lake bottom is interpreted to be produced by discontinuous algal mats.

Station locations and elevations were obtained using a Trimble GeoXT differential Global Positioning System instrument. The GeoXT receiver uses the Wide Area Augmentation System (WAAS), which, combined with a base-station and postprocessing using Continually Operated Reference Station (CORS) satellites, results in submeter horizontal and vertical accuracy.

Terrain corrections, which account for the variation of topography near a gravity station, were computed using a combination of manual and digital methods. Terrain corrections consist of a three-part process: the innermost or field-terrain correction, innerzone-terrain correction, and outerzone-terrain correction. The innermost-terrain corrections were estimated in the field and extend from the station to a radial distance of 68 m, equivalent to Hayford and Bowie's (1912) zone B. Innerzone-terrain corrections were estimated from digital elevation models (DEMs) with 10- or 30-m resolutions derived from USGS 7.5' topographic maps and extend from 68 m to a radial distance of 2 km (D. Plouff, USGS, unpub. software, 2006). Outerzone-terrain corrections, from 2 km to a radial distance of 167 km, were computed using a DEM derived from USGS 1:250,000-scale topographic maps and an automated procedure based on geographic coordinates (Plouff, 1966; Plouff, 1977; Godson and Plouff, 1988). Digital terrain corrections are calculated by computing the gravity effect of each grid cell in the DEM using the distance and difference in elevation of each grid cell from the gravity station.

15
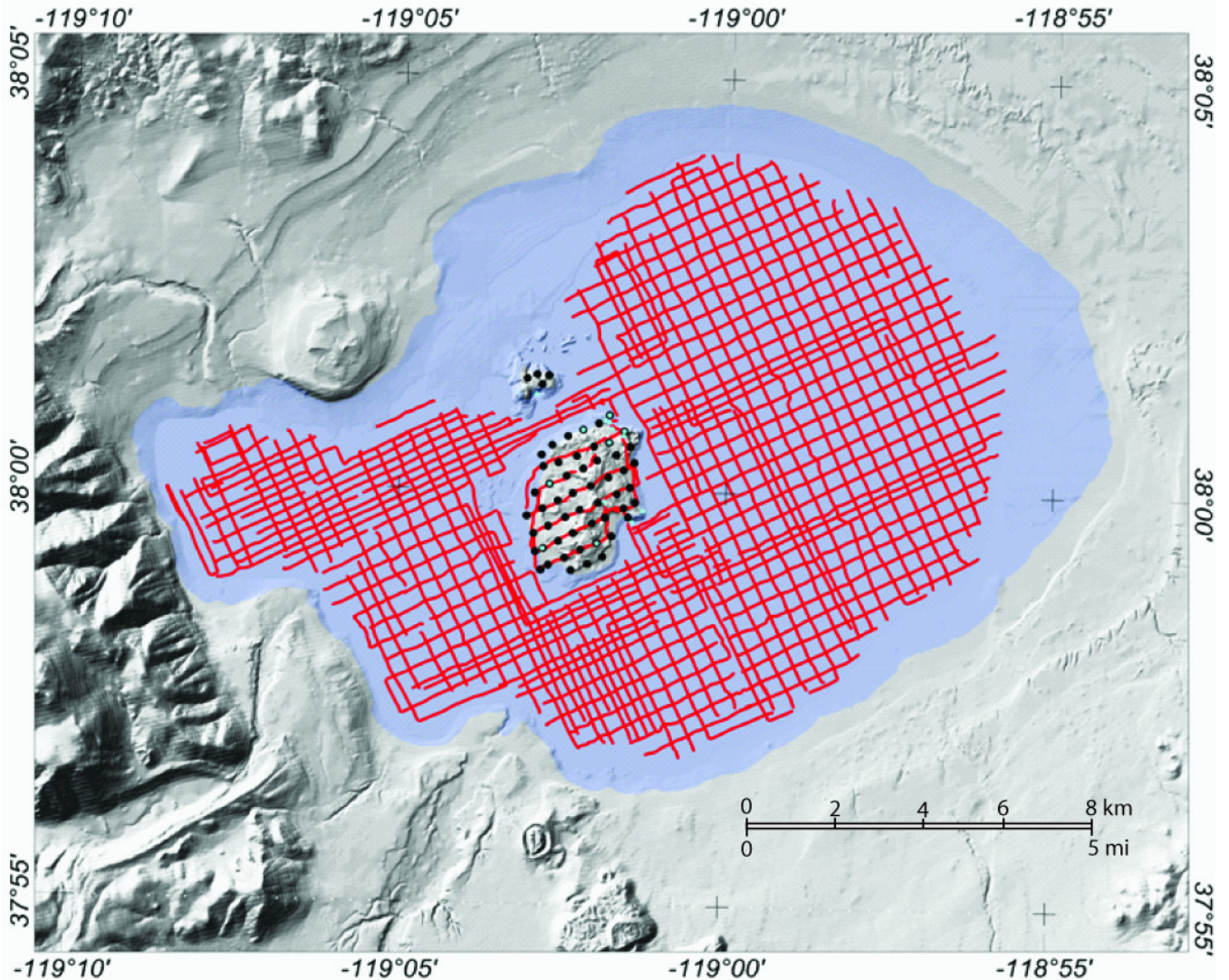
Figure 12. Map showing locations of ship-borne magnetic survey, ground magnetic survey, gravity survey, and rock-sample sites for physical property measurements. Red line-ship-borne and ground magnetic traverse; black dots-gravity station location; blue dots-rock sample location.

Physical-Property Data

We collected rock samples on Paoha and Negit Islands and recorded data for them that include station identifier, geographic coordinates, rock type, density, and magnetic susceptibility. Densities were determined using the buoyancy method with an electronic balance, and magnetic susceptibility measurements were made using a Kappameter KT-5. Grain, saturated-bulk, and dry-bulk densities were computed for each sample by weighing the sample in air (Wa), saturated and submerged in water (Ww), and saturated and weighed in air (Was) using the following formulas, where weights were measured in grams:

Grain density $= 1,000$ kg/m^3 * Wa/(Wa-Ww),
Saturated-bulk density $= 1,000$ kg/m^3 * Was/(Was-Ww), and
Dry-bulk density $= 1,000$ kg/m^3 * Wa/(Was-Ww).

References Cited

Barnes, D.F., Oliver, H.W., and Robbins, S.L., 1969, Standardization of gravimeter calibrations in the Geological Survey: Eos (American Geophysical Union Transactions), v. 50, no. 10, p. 626–627.

Blakely, R.J., 1995, Potential theory in gravity and magnetic applications: New York, Cambridge University Press, 441 p.

Bursik, M., 1989, Late Quaternary volcano-tectonic evolution of the Mono Basin, eastern California: California Institute of Technology, Ph.D. dissertation, 270 p.

Bursik, M., and Sieh, K., 1989, Range Front faulting and volcanism in the Mono Basin, eastern California: Journal of Geophysical research, v. 94, p. 15587–15609.

Dobrin, M.B., and Savit, C.H., 1988, Introduction to geophysical prospecting (4th ed.): New York, McGraw-Hill, 867 p.

Finlayson, D.P., Triezenberg, P.J., and Hart, P.E., 2010, Geophysical surveys of the San Andreas and Crystal Springs Reservoir System including seismic-reflection profiles and swath bathymetry, San Mateo County, California: U.S. Geological Survey Open-File Report 2010-1030.

Godson, R.H., and Plouff, Donald, 1988, BOUGUER version 1.0, a microcomputer gravity-terrain-correction program: U.S. Geological Survey Open-File Report 88–644–A, Documentation, 22 p.; 88–644–B, Tables, 61 p. 88–644–C.

Hayford, J.F., and Bowie, William, 1912, The effect of topography and isostatic compensation upon the intensity of gravity: U.S. Coast and Geodetic Survey Special Publication no. 10, 132 p.

Hildreth, Wes, 2004, Volcanological perspectives on Long Valley, Mammoth Mountain, and Mono Craters; several contiguous but discrete systems: Journal of Volcanology and Geothermal Research, v. 136, p. 169–198.

Hill, D.P., and Prejean, S., 2005, Magmatic unrest beneath Mammoth Mountain, California: Journal of Volcanology and Geothermal Research, v. 146, p. 257–283.

Huber, N.K., and Rinehart, C.D., 1967, Cenozoic volcanic rocks of the Devils Postpile Quadrangle, eastern Sierra Nevada, California: U. S. Geological Survey Professional Paper 554–D, 28 p.

International Union of Geodesy and Geophysics, 1971, Geodetic reference system 1967: International Association of Geodesy Special Publication no. 3, 116 p.

Jachens, R.C., and Roberts, C.W., 1981, Documentation of a FORTRAN program, 'isocomp,' for computing isostatic residual gravity: U.S. Geological Open-File Report 81–574, 26 p.

Jenkinson, I.R., and Sun, J., 2010, Rheological properties of natural waters with regard to plankton thin layers—a short review: Journal of Marine Systems, v. 83, p. 287–297.

Lodolo, E., Baradello, L., Darbo, A., Caffau, M., Tassone, A., Lippai, H., Lodolo, A., De Zorzi, G., and Grossi, M., 2012, Occurrence of shallow gas in the easternmost Lago Fagnano (Tierra del Fuego): Near Surface Geophysics, v. 10, no. 2, p. 161–169

Marlow, M.S., Hart, P.E., Carlson, P.R., Childs, J.R., Mann, D.M., Anima, R.J., and Kayen, R.E., 1996, Misinterpretation of lateral acoustic variations on high-resolution seismic reflection profiles as fault offsets of Holocene bay mud beneath the southern part of San Francisco Bay, California: Marine and Petroleum Geology, v. 13, no. 3, p. 341–348.

Melack, J.M., and Jellison, R., 1998, Limnological conditions in Mono Lake; contrasting monomixis and meromixis in the 1990s: Hydrobiologia, v. 384, p. 21–39.

Morelli, C., ed., 1974, The International Gravity Standardization Net 1971: International Association of Geodesy Special Publication no. 4, 194 p.

Pelagos Corporation, 1987, A bathymetric and geologic survey of Mono Lake, California, for Department of Water and Power, Los Angeles, California: San Diego, California, Pelagos Corporation, 38 p. plus map appendixes.

Plouff, Donald, 1966, Digital terrain corrections based on geographic coordinates: Geophysics, v. 31, no. 6, p. 1208.

Plouff, Donald, 1977, Preliminary documentation for a FORTRAN program to compute gravity terrain corrections based on topography digitized on a geographic grid: U.S. Geological Survey Open-File Report 77–535, 45 p.

Raumann, C.R., Stine, S., Evans, A., and Wilson, J., 2002, Digital bathymetric model of Mono Lake, California: U.S. Geological Survey Miscellaneous Field Studies Map MF–2393, 10 p. (Also available at *http://pubs.usgs.gov/mf/2002/2393/.*)

Richards, S.D., 1998, The effect of temperature, pressure, and salinity on sound attenuation in turbid seawater: Journal of the Acoustical Society of America, v. 103, no. 1, p. 205–211.

Ritchie, A.C., Finlayson, D.P., and Logan, J.B., 2010, Swath bathymetry surveys of the Monterey Bay area from Point Año Nuevo to Moss Landing, San Mateo, Santa Cruz, and Monterey Counties, California: U.S. Geological Survey Data Series 514.

Scholl, D.W., Von Huene, R., St-Armand, P., and Ridlon, J., 1967, Age and origin of topography beneath Mono Lake, a remnant Pleistocene lake, California: Geological Society of America Bulletin v. 78, p. 583–600.

Sieh, K., and Bursik, M., 1986, Most recent eruption of the Mono Craters, eastern central California: Journal of Geophysical Research, v. 91, p. 12539–12571.

Stine, S., 1990, Late Holocene fluctuations of Mono Lake, eastern California: Paleogeography, Paleoclimatology, Paleoecology, v. 78, p. 333–381.

Swick, C.A., 1942, Pendulum gravity measurements and isostatic reductions: U.S. Coast and Geodetic Survey Special Publication 232, 82 p.

Wood, S.H., 1983, Chronology of late Pleistocene and Holocene volcanics, Long Valley and Mono Basin geothermal areas, eastern California: U.S. Geological Survey Open-file Report 83–747, 76 p.